

Modelling Tension and Torque Properties of Fibre Ropes and splices

C M Leech, Reader in Mechanical Engineering, UMIST,
PO Box 88, Manchester, M60 1QD, ENGLAND

and

J W S Hearle, M S Overington and S J Banfield,
Tension Technology International Ltd.,
Lloyds Wharf, 2 Mill Street, London, SE1 2BD, ENGLAND

ABSTRACT

Traditionally rope design and selection has been an empirical craft, but this is no longer adequate when the choices have multiplied into hundreds of thousands and severe engineering demands apply to some uses, especially for long periods off-shore.

This paper outlines a quasi-static analysis which has been developed for structured ropes and embodied in computer codes for prediction of the quasi-static and long-term properties of ropes. In this fundamental stage the codes compute tension and torque from their dependence on elongation and twist, thereby allowing the breakage of both ropes and splices to be predicted and improved designs developed.

KEYWORDS : Ropes, Splices, Modelling,
Response, Strength, Tension,
Torque

INTRODUCTION

Fibre ropes have been used for thousands of years, but recent advances have increased the potential for civil engineering applications in the oceans. In turn, this has stimulated research into the applied mechanics of ropes and the development of engineering design tools. Computer modelling is needed both to enable manufacturers to optimise constructions and investigate novel structures and to enable engineering users to make the right design decisions.

The need to bind short natural fibres, such as hemp, sisal and cotton, together by frictional forces led to traditional twisted structures, predominantly three-strand ropes. This requirement ceased from the 1950's onwards when continuous filament yarns of nylon, polyester and polypropylene became available. One consequence was the invention of a range of new fibre rope constructions: lower twist wire-rope types and parallel assemblies of sub-ropes; braided forms; and

parallel-lay ropes. These first synthetic fibres have strengths of around 1 GPa, about half that of steel, but, because of their low density, they are about three times stronger on a weight basis. A new generation of high-performance fibres - aramid (Kevlar, Twaron, Technora), HMPE (Spectra, Dyneema) and LCAP (Vectran) - have strengths in the range 2 to 4 GPa and are up to ten times stronger than steel on a weight basis. In stiffness, these fibres range from under 5 GPa for nylon to around 200 GPa for aramids: this is still slightly lower than steel, but, on a weight basis is five times higher.

The overall position is now that polypropylene is used for lower-cost commodity ropes; nylon is preferred where extensibility and energy absorption are required; polyester provides good strength and stiffness at a moderate cost; aramid, HMPE and LCAP fibres provide higher strength and stiffness, though the creep of HMPE militates against long-term uses under high loads. All these fibres have the toughness to be used as fine filaments (about 10 μm in diameter) in ropes. Glass and carbon fibres also have high strength and stiffness, but are too brittle to be used unprotected, though they can be used as pultruded rods.

New rope designs are leading to more efficient utilisation of fibre properties in the total structure. However, so far the development of constructions has mainly been by practical innovation, and the empirical evaluation of performance has been limited by the high cost of testing. There has been a lack of tools for the optimisation of design, although, if the fundamental basis is understood, modern computing power should make this possible. Furthermore engineers are naturally reluctant to use new materials and constructions in demanding situations, unless their performance can be adequately predicted.

This paper presents an account of computer codes for prediction of the quasi-static and long-term properties of ropes. Codes have been developed with facilities for

both unstructured (parallel-lay) and structured ropes, but this paper will be limited to twisted rope structures. Particular attention is paid to "wire-rope" and multi-rope constructions, which have strength conversion efficiencies similar to parallel-lay ropes and are better suited to a number of applications. The inclusion of splices as terminations of twisted ropes introduces methods which would also be applicable to braided ropes. In addition to the prediction of the relations between tension, length, torque and twist, this paper will also include methods for the computation of internal forces and heat generation, which are needed for the long-term response discussed in an associated paper.

Within the confines of a short paper, it is only possible to give an outline of the theoretical basis, which, in a full treatment would require detailed discussion of the underlying assumptions and mathematical and computational procedures. The validity of the procedures is shown here by the examples of applications.

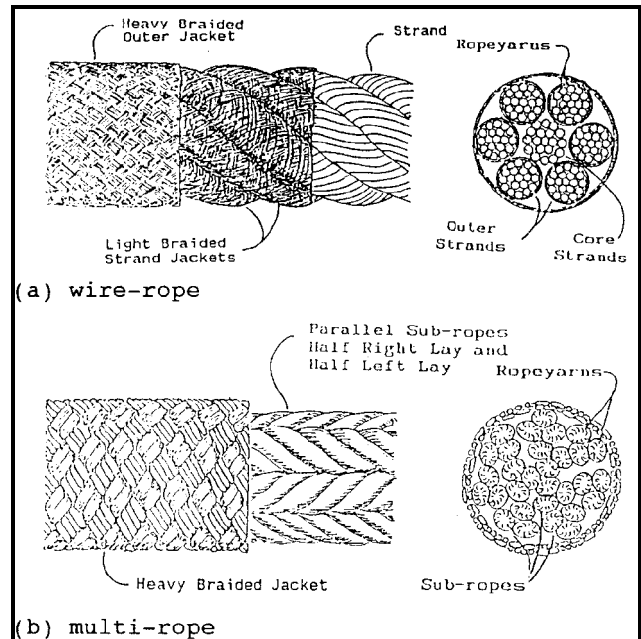


Figure 1 :Rope constructions

MODELLING PRINCIPLES

Rope geometry and fibre content

The modelling of rope geometry follows a hierarchical approach with a number of levels, which mirrors the manufacturing process. Typical sequences are shown in Table 1 and the constructional differences are illustrated in Fig. 1. Although, in principle, all levels could be included in the modelling, in practice the properties of either the "textile yarn" or the "rope yarn" are taken as the starting point. These are specified in terms of: linear density (mass/length); density, which determines diameter and depends on fibre density and packing factor within the yarns; tensile stress-strain properties; and coefficient of friction. Different fibres may be combined within the same rope.

ROPE TYPE:	WIRE-ROPE	MULTI-ROPE
Fibre manufacturer	filament	filament
Rope maker	textile yarn	textile yarn
	strand	strand
	rope	sub-rope
		rope

Table 1 Structural levels in ropes

At each structural level (e.g., a strand), the next lower level form (e.g., the rope yarn) follows a uniform helical path around a central axis as shown in Fig. 2. This means that an individual filament will

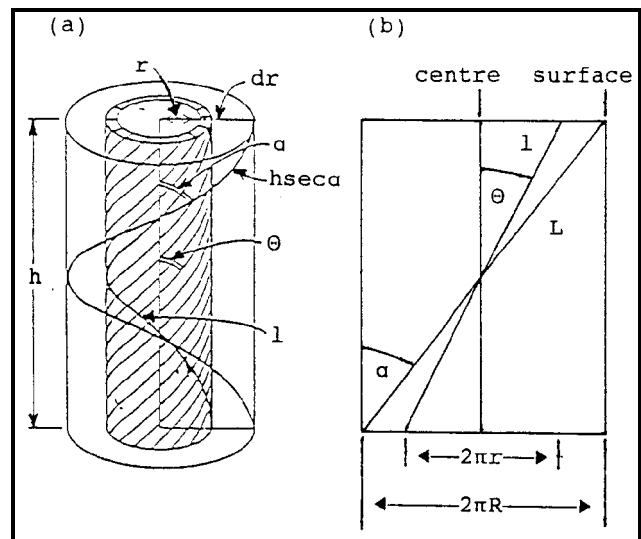


Figure 2 : Twist geometry, (a) Components follow helical paths round concentric cylinders and (b) Opening-out cylinder flat defines geometrical and trigonometrical relations.

follow a complicated path determined by the multiplicity of helices. However, since the properties of each level are determined separately and used as input to the next higher level, these complications are avoided and the only geometry that needs to be defined is that of Fig. 2, with relations derived from the triangles in the "opened-out" diagram. The consequences on twist at a lower level of the subsequent twisting at a higher level have to be taken into account.

Packing involves both qualitative and quantitative aspects. Three forms of arrangement of components, shown in Fig. 3, are considered: in "packing" geometry, the elements are in circular layers where the contact stresses act radially towards the central axis; in "wire-rope" geometry, circular layers are self-supported by circumferential pressures where contact stresses act circumferentially within the assembly; in "wedge" geometry the components are deformed into pieces bound by segments of radii and arcs, and generate contact forces both radially and circumferentially. For each geometry, there is a packing factor in the stress-free state, which may be reduced by lateral pressures developed under tension.

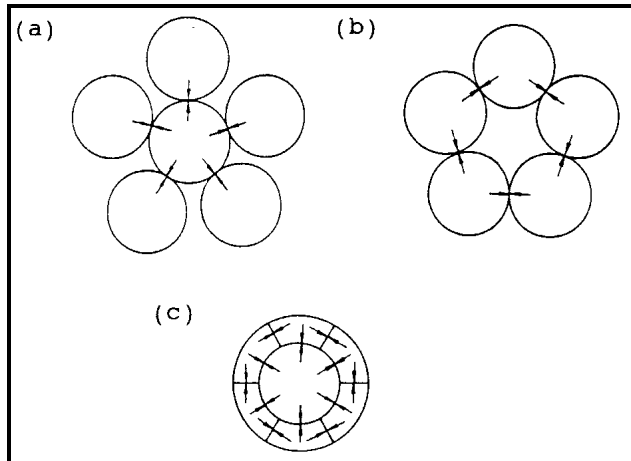


Figure 3 : Cross-sectional geometry, (a) packing geometry, (b) wire-rope geometry and (c) wedge geometry.

Variability in structure and fibre properties may have an appreciable influence on rope strength, especially in low twist highly lubricated ropes.

Rope deformation

The basic deformation assumption is that planes perpendicular to the axis of the helical structure within each component remain planar and perpendicular to that axis. The circular cross-sections at either end of the element in Fig. 2 thus move farther apart due to extension, rotate relative to one another due to twist, and reduce in area either to keep the volume constant or to allow for compression. Analysis by differential geometry then gives expressions for the elongation of the lower level components, and keeps track of the sequence of imposed deformations through the several layers of the structure.

In order to introduce frictional effects, it is necessary to consider slip at contact points. The modes of slip are numerous, and their magnitude must be found from the differential geometry of deformation. Those identified as the more important and taken into account as appropriate,

particularly in the later fatigue studies, are illustrated in Fig. 4 and listed as follows: modes 1 and 2, axial sliding between components due to stretching and twisting of the structure; mode 3, rotational slip, which is an end-effect; mode 4, scissoring at crossovers; mode 5, sawing at crossovers; mode 6, bulk compression or dilation. There is also component distortion, which has not yet been explicitly treated, but is implicitly catered for by providing treatments for both the initial, cylindrical, and final, wedge, shaped construction geometries.

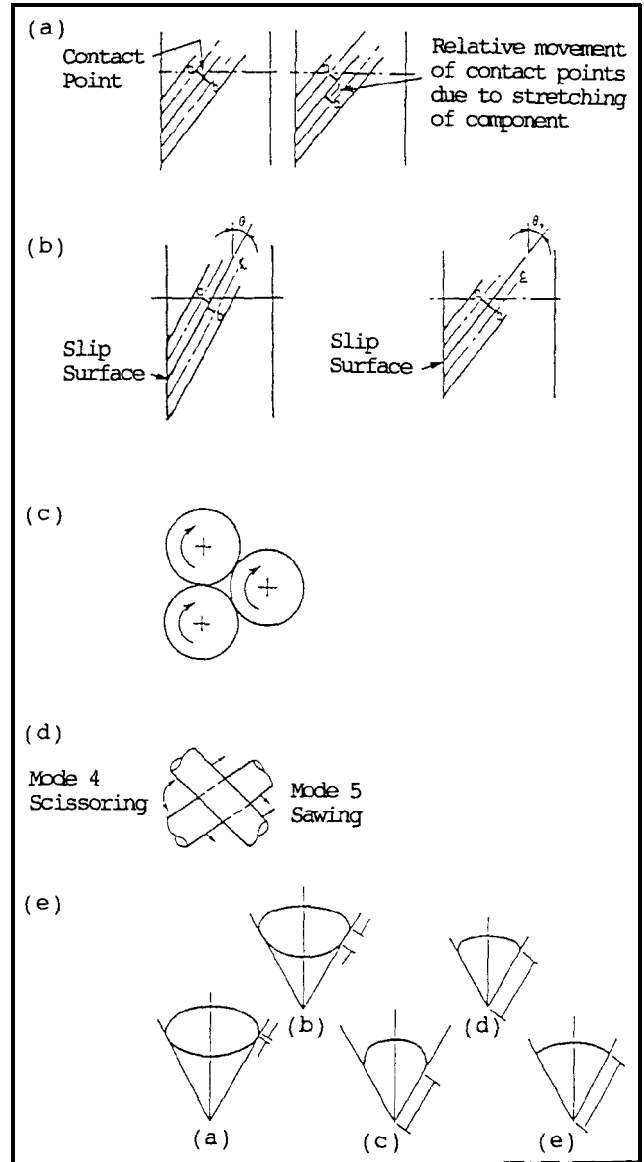


Figure 4 : Modes of slip. (a) Mode 1 stretching, (b) Mode 2 twisting, (c) Mode 3 rotating, (d) Mode 4 scissoring and mode 5 sawing, (e) Mode 6 distortion. Progressive distortion of strand from (a) to (e).

The scissoring, sawing and bulk compression modes of slip have been identified as significant in fatigue failure mechanisms

but not in their effect on rope loads, as they are associated with small displacements.

Rope mechanics

The analysis is based on the Principle of Virtual Work:

$$P \cdot L + T \cdot N = U \tag{1}$$

where **P** is tension and **L** is elongation, **T** is torque and **N** is twist, and **U** is strain energy.

Because the rope is composed of an extremely large number of fine filaments, bending and torsional effects in the input components can be neglected. It is only necessary to take account of elongation energy obtained by integration of the tensile stress-strain properties, which can be measured on yarns in extension and recovery. Effects at higher levels come naturally into the analysis.

Application of virtual displacements then gives the expressions for tension and torque:

$$P = 3F_c l_{oc} (M_c / ML) \quad T = 3F_c l_{oc} (M_c / MN) \tag{2}$$

where **F_c** is the axial load in the component as a function of **L, N**, **l_{oc}** is the reference length of the component, and **c** is the strain in the component.

In order to determine contact forces, it is necessary to introduce a virtual change in the helix radius **a**. The contact force per unit length is then given by expressions similar to the above involving **(M_c / Ma)**. The frictional force is given by multiplying the contact force by the coefficient of friction. The frictional contribution to the deformation energy, which must be added into the computed work, is the product of friction force and displacement at the contacts as derived from the rope deformation. The only significant contribution, and even that is small, comes from the axial sliding mode.

The analysis outlined above enables tension and torque in ropes to be calculated as functions of elongation and twist. Breakage occurs when the input components, normally yarns, reach their breaking extension. Except in unusual constructions, this will indicate the maximum load, namely the rope strength, and, in practice, will usually be the trigger for catastrophic failure.

Heat generation and conduction

Heat generation during rope deformation comes from two sources: dissipation within fibres calculable from the hysteresis or loss factor in the yarn stress-strain behaviour; frictional losses calculated as above. Both can be derived from the mechanical analysis.

In repeated cycling, which is treated in more detail in the associated paper, the heat generation causes an increase in temperature.

If the rope is regarded as a circular cylinder of constant thermal diffusivity (density x specific heat / thermal conductivity), Green's functions in the literature can be used to model the change with time of the temperature distribution due to a heat source located at any point in the cross-section. The effects are additive, so the overall change in temperature can be computed by adding the contributions from all the fibre and contact deformations in the rope structure, which are present in the analysis.

Splice geometry and mechanics

Although terminations do not contribute appreciably to the elongation of a long rope system, they may be a point of failure. The present analysis has therefore been extended to include some commonly used eye splices. Splice geometry consists of an interlacing, or braiding, of tuck (**T**) strands from the free end of the rope under and over (**S**) strands from the main rope. Typical splices are shown in Fig. 5.

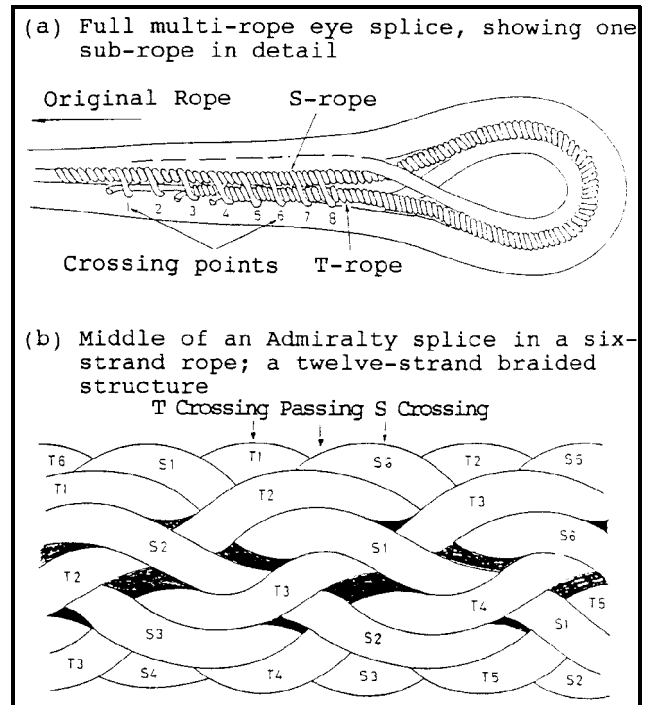


Figure 5 :Splice geometry

Specification of the differential geometry of the braided structure and the application of the principle of virtual work enable the tensions to be calculated at different locations in the splice. The most severe stress comes at the end of the splice, where the whole rope tension is borne by the (**S**) strands in a disturbed geometry, since the free tuck ends can carry no load. Back along the splice there is a progressive transfer of load from (**S**) to (**T**) strands until it is equally shared. The analysis enables the splice strength to be calculated.

In addition, the magnitude of the scissoring friction mode, which is important due to the trellising action in a braided structure, can be determined. This is significant in fatigue failure, discussed in the associated paper.

COMPUTATION

The analysis outlined above has been coded in and for the PC environment, using BORLAND's Turbo-Pascal language, in a way which is easy for the user to implement. The input requirements fall into two parts, which include provision for slack strain variability.

First, the user must define the rope structure. Essentially, this consists of specifying the number of components at each level along with the twist inserted and the nature of the packing at that level. Because of the number of levels provided, this can be a lengthy, but straightforward, procedure. Splice structure parameters must also be given if splice analysis is required.

Second, the dimensional, tensile and frictional properties of the lowest level components must be provided. Most are single parameters, but the nonlinear stress-strain relations are defined in the codes by the coefficients of fourth order polynomials, which can be derived from test data.

With the input requirements satisfied, numeric and graphical predictions of rope response can be obtained for direct or cyclic loading between any selected pair of applied rope extensions. In the process of predicting the overall rope response, predictions of the response of each and every component are produced and these may be interrogated at leisure.

Comparison with experiment

A number of measurements of tension and torque developed in ropes, strands and yarns have been performed in order to confirm the validity of the theory and computer codes.

Fig. 6 shows the good correlation between theory and experiment for all three levels (the rope itself, a sub-rope and a sub-rope strand) of a Multi-Rope polyester.

Fig. 7 shows how the codes were used to improve the performance of a 7 strand aramid rope. **E1** is the experimental result from the rope as originally manufactured. The theoretical prediction **T** indicated the original manufacturing was incorrect. Rope manufacture was improved in the re-make to yield the experimental result **E2**, which agrees with the prediction.

Fig. 8 shows how the mean torque - twist response of a bedded-in rope can be predicted, and agrees with experimental results.

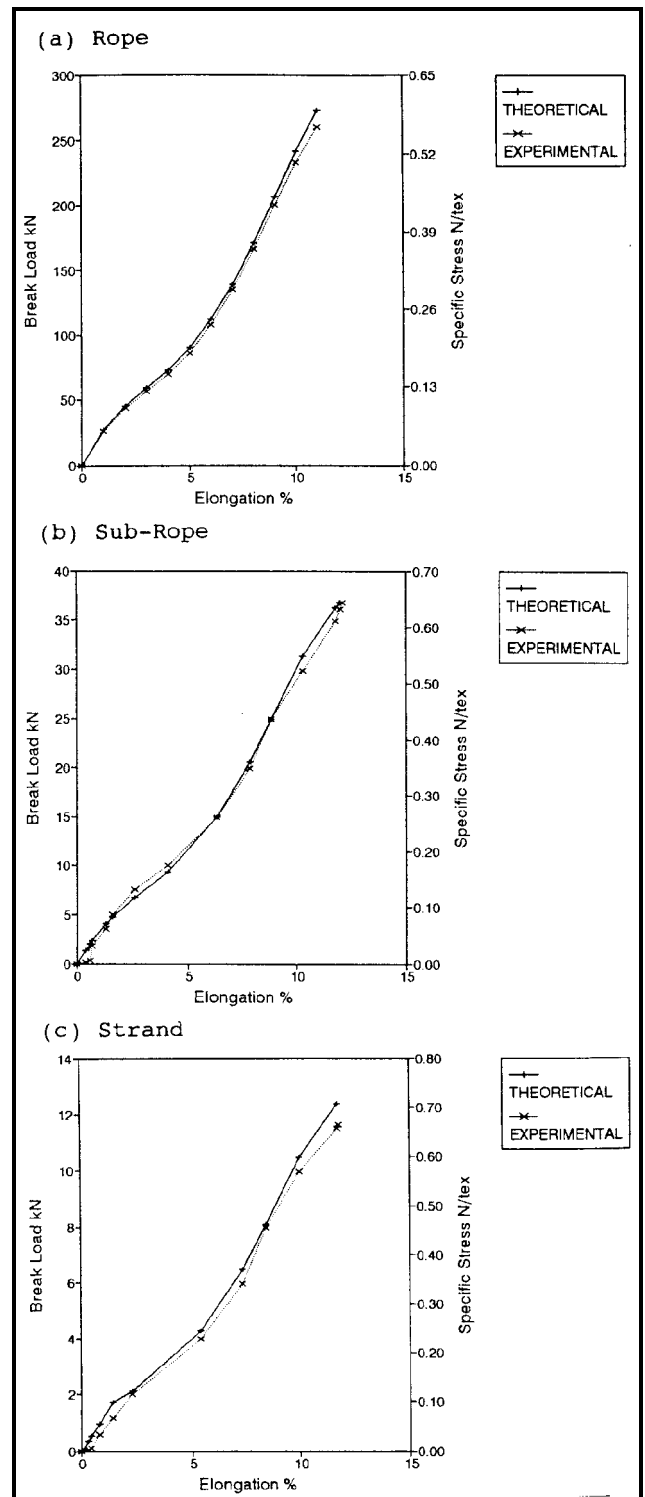


Figure 6 : Experimental and theoretical load- elongation comparison for Multi-Rope Polyester.

These results demonstrate that the developed codes give useful predictions, so that they can be used with confidence to evaluate the properties of candidate ropes or investigate design changes.

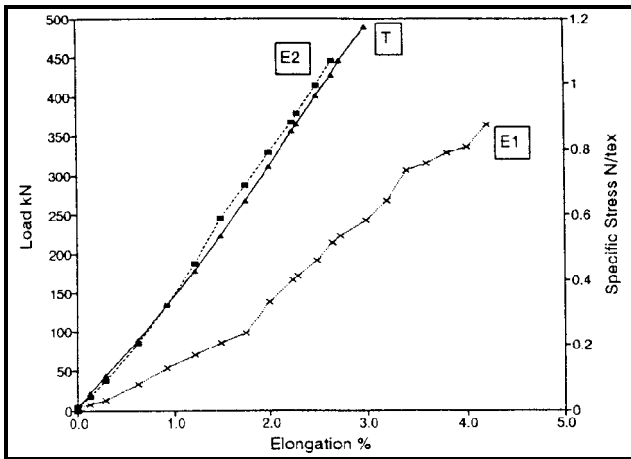


Figure 7 : Load - elongation of 7 Strand Aramid : E1 and E2 are experimental results for incorrectly and correctly made ropes, respectively ; T is theoretical prediction.

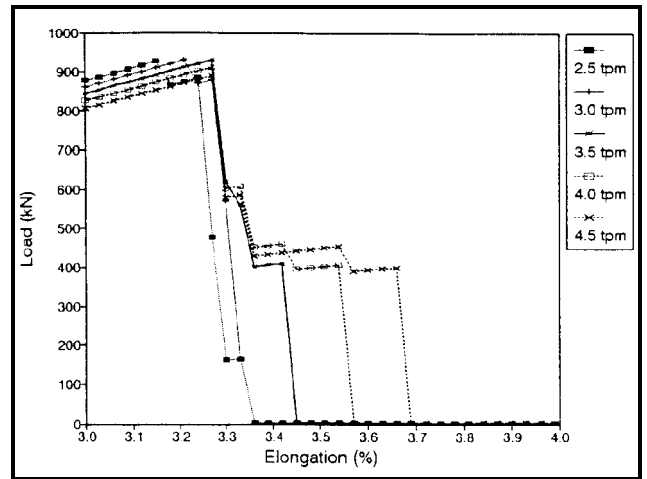


Figure 9 : Effect of outer layer twist on 36 strand aramid rope

load bearing components break together, at an outer layer twist of . 3.5tpm. The uneven sharing of load at other twist levels has fatigue implications.

Fig. 10 shows the effect of replacing the aramid load bearing elements of a 7 strand rope with polyester. The core rope yarn of the core strand of the aramid rope is polyester, which explains why it is still predicted to carry a small load up to 12% elongation.

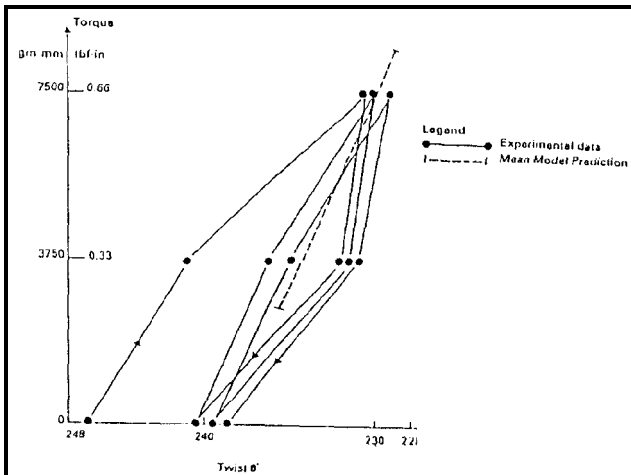


Figure 8 : Torque - Twist of Multi-Rope Polyester Strand

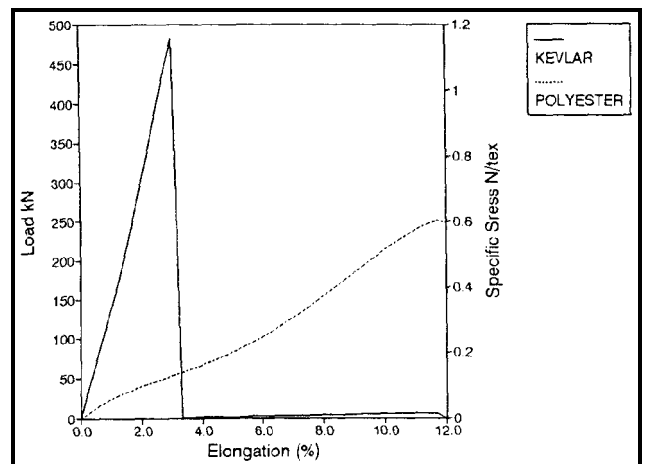


Figure 10 : Effect of Constituent material on 7 strand

Fig. 11 shows how the codes can help to design-out undesirable rope characteristics, i.e., in this instance to achieve torque balance. The unbalanced and balanced wire rope constructions are 7 strand (2 layer) and 36 strand (4 layer) aramid ropes respectively.

Fig. 12 shows the relatively small effect of friction in a Multi-Rope polyester.

Fig. 13 depicts the hysteresis due to load cycling in a 7 strand aramid. Heat generated is given by the enclosed area.

Parametric studies

Another way in which the codes can be used is to investigate the sensitivity of rope performance to changes in construction and material properties.

Fig. 9 shows the significant effect on ultimate rope modulus of changing the outer layer twist in a 36 strand (4 strand layer construction) while keeping all other parameters fixed. The modulus, as indicated by stress at 3% elongation, decreases by about 10% when the twist level increases from 2.5 to 4.5tpm. The change of outer layer twist from 2.5tpm to 3.5tpm increases break strain by .5%, with little change in peak load, but a further change to 4.5tpm reduces break strength by .5%, with little change in break strain. It can be seen that the optimal behaviour will be achieved when the principal

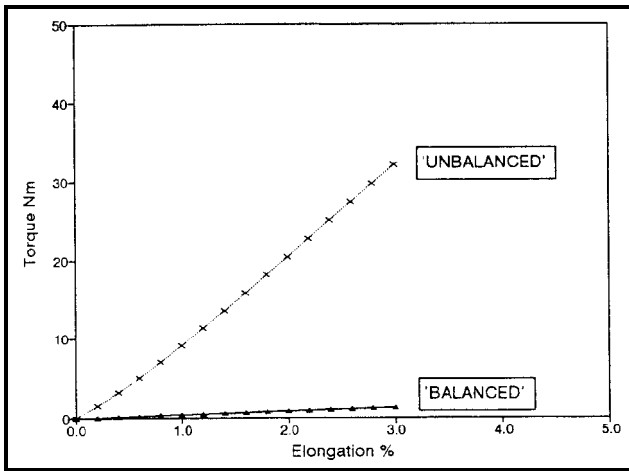


Figure 11 : Comparative Torque Balance between Aramid wire rope designed with and without attention to torque balance.

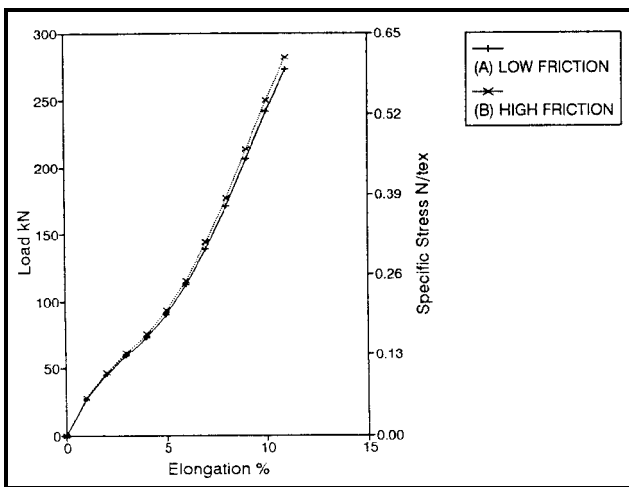


Figure 12 : Effect of Friction on Multi-Rope Polyester; (A) $\mu = 0.1$, 0.1, 0.1 modes 1, 2 and 3, (B) $\mu = 1.0$ modes 1 and 2.

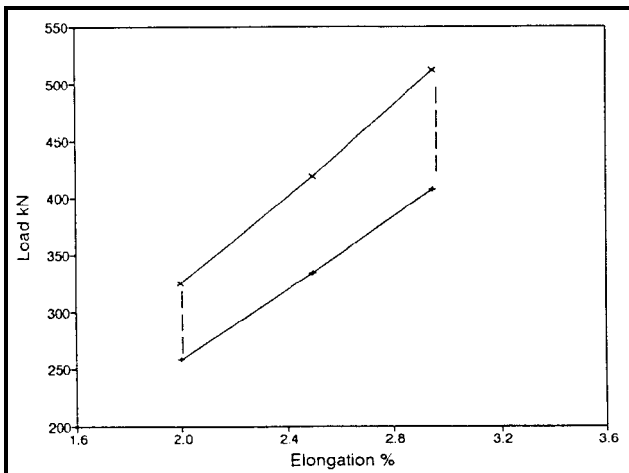


Figure 13 : Hysteresis due to Load Cycling on 7 Strand Aramid

CONCLUSION

Although there are inevitable assumptions and approximations, some for reasons of mathematical simplification and some due to uncertainties in rope construction, the analysis of structured ropes outlined in this paper, and associated codes for unstructured parallel-lay ropes also developed, enable worthwhile predictions of the response of ropes to be calculated. Tension and torque can be computed in their dependence on elongation and twist, and the breakage of both ropes and splices predicted. These codes have already been used to design ropes for floating production system mooring studies and to assist ropemakers with new rope designs.

In addition to the quasi-static response (individual cycles of extension and recovery), which is the main concern of this paper, these codes provide necessary input to the modelling of long-term fatigue behaviour discussed in the associated paper.

ACKNOWLEDGMENT

The financial support of the US Navy, through NCEL contract N.62474.87.C.3073, to package this analysis into the computer program GEN-ROPE and the advice and encouragement of Dr Francis Liu is gratefully acknowledged.

We also gratefully acknowledge the advice of M R Parsey, Prof R E Hobbs (including supervision of the experimental work on torque measurements at Imperial College, London), and J F Flory (including studies of splice geometry).

REFERENCES

Hearle, J.W.S., Parsey, M.R., Overington M.S. and Banfield S.J. (1993). "Modelling the Long Term Performance of Fibre Ropes", *Third (1993) International Offshore and Polar Engineering Conference, Singapore*.